DEVELOPMENT OF A THERMIONIC TRIODE RF GUN*

K. Masuda#, T. Shiiyama, T. Kii, H. Ohgaki, Inst. Advanced Energy, Kyoto Univ., Uji, Kyoto 611-0011, Japan
K. Kanno, E. Tanabe, AET Inc., Kawasaki, Kanagawa 215-0033, Japan

Abstract

A thermionic triode rf gun is being developed to mitigate the adverse effect of electron back-bombardment onto the cathode inherent in conventional rf guns. An coaxial rf cavity with a thermionic cathode on the inner rod of the coax was designed and fabricated, which is to be installed in an existing conventional rf gun to configure the rf triode structure. The rf coupler geometry between the coaxial cavity and the rf waveguied was designed by use of a 3-D electromagnetic field solver. Numerical comparisons were made between two candidates, namely W and LaB_6, for the thermionic cathode material. As the result, unlike in the conventional rf gun, W cathode is found to enable a longer macro-pulse duration for the same back-bombardment power. Expected macro-pulse duration by the triode rf gun is twice as long as the conventional gun with ~10 times higher peak current without degradation in emittance.

INTRODUCTION

Thermionic rf guns can produce electron beams with high brightness and high averaged current (high micro-pulse repetition rate) in a compact system using resonant rf cavities and a thermionic cathode. These properties make the thermionic rf guns well suited for the use in high averaged power FELs. In a conventional thermionic rf gun, however, the back-bombardment of the electrons causes the heating of the cathode surface, which eventually leads to rapid energy drop of the output beam and limits the macro-pulse duration by changing the thermal electron emission [1-3]. Several methods such as the use of transverse magnetic fields [1,4] and the rf input control for compensating time-varying beam-loading [5-7] have been applied to mitigate this problem. The maximum pulse duration of the rf gun operation is, however, limited to several microseconds, while a longer macro-pulse duration would be desired for the FEL operation.

For this purpose, we have proposed what we call a triode rf gun [8], in which an additional coaxial rf cavity with a thermionic cathode set on its inner rod replaces the conventional cathode in an rf gun. A numerical study showed that the rf triode concept can reduce the back-bombardment power drastically, and at the same time reduce the longitudinal emittance of the output beam [9]. A wehnelt structure was designed by 2-D particle-in-cell (PIC) simulations [10] in order to suppress the transverse emittance increase by compensating the inherent defocusing effect induced by the rf triode [10]. Also, the cavity parameters, namely the quality factor and the coupling coefficient of the additional coaxial cavity with an rf feed coaxial cable were determined based on an equivalent circuit model to ensure both the induction of the required cavity voltage and a wide frequency acceptance [11].

This paper describes design and development of a prototype coaxial cavity to be installed in a 4.5-cell S-band thermionic rf gun in the KU-FEL [12]. The rf coupler design made by use of a 3-D electromagnetic field solver is presented. Also, comparisons are made between candidate cathode materials in terms of temporal evolution of the cathode surface temperature rise induced by the electron back-bombardment by use of a 1-D time-dependent code [6].

OVERVIEW OF TRIODE RF GUN

Figure 1 shows a schematic cross-sectional view of the triode rf gun. An existing 4.5-cell conventional rf gun, and an additional coaxial cavity (see a photo in Fig. 2) constitutes the triode rf gun. A thermionic cathode of 2-mm diameter is set on the inner rod of the coaxial cavity. Thermal electrons are then extracted by an rf field of ~20 kV/m induced at a short accelerating gap of ~3 mm and injected into a successive rf gun main cavity through 2-mm aperture, while the rf fields in the two cavities are cut off by the small aperture.

Figure 3 shows the cavity geometry designed by the 2-D PIC code and eigenmode pattern in the vicinity of the thermionic cathode. A steep wehnelt electrode (40 deg. with respect to the axis, see also photo in Fig. 4) is adopted to minimize the transverse emittance by compensating the inherent defocusing effect induced in

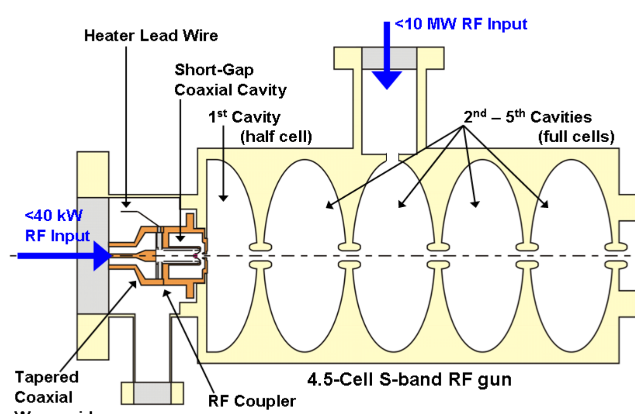

Figure 1: Schematic cross-section of a thermionic triode rf gun.

*Work supported by the Grant-in-Aid for Scientific Research of the Ministry of Education, Culture, Sports, Science and Technology of Japan (#18686010).
#masuda@iae.kyoto-u.ac.jp

Figure 2: Coaxial cavity to be installed in an existing conventional rf gun.

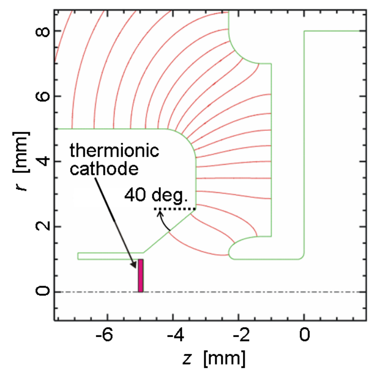

Figure 3: Cylindrically symmetric eigenmode pattern in the vicinity of the cathode in the coaxial cavity.

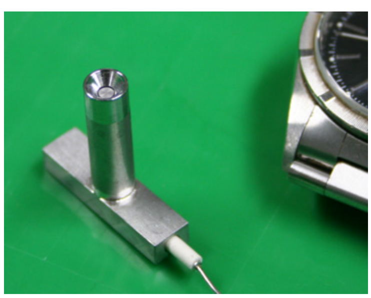

Figure 4: Tungsten cathode of 2-mm diameter with the wehnelt electrode.

the rf triode configuration [11]. The expected properties of the output beam by the 2-D PIC code are summarized in Table 1 in the following section.

RF SYSTEM AND RF COUPLER DESIGN

As shown schematically in Fig. 1, the coaxial cavity is fed with an rf input power of ~40 kW through a tapered coaxial waveguide and an rf coupler both of which is set in vacuum.

The triode rf gun does not require an additional rf source, because the rf power required to drive the additional coaxial cavity is moderate and small compared with the power for the original rf gun. Thus, a 20 dB coupler was installed as seen in Fig. 5 along the waveguide between the rf gun main cavities and an existing 10 MW klystron to feed them, followed by a

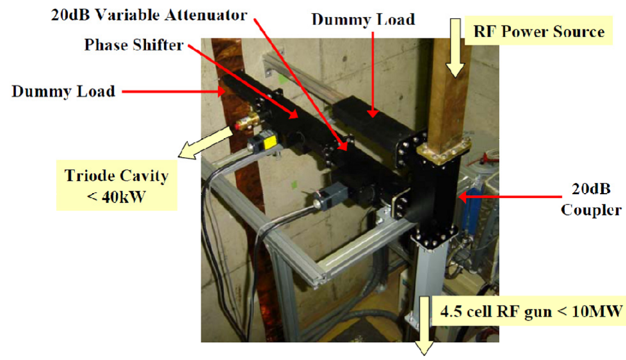

Figure 5: RF waveguide components of the rf feed system for the triode rf gun.

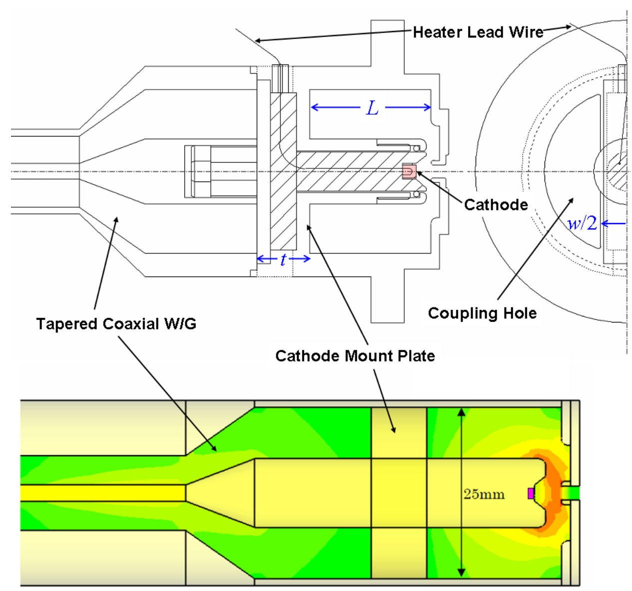

Figure 6: RF coupler geometry and calculated electric field distribution.

variable attenuator and a phase shifter also show in Fig. 5, to control the amplitude and phase of the rf voltage in the coaxial cavity.

Cross-sectional views of the rf coupler of the coaxial cavity with the tapered coaxial waveguide are shown in Fig. 6, together with a calculated electric field distribution. As shown in the figure, the inner rod of the coax is supported by the cathode mount plate. The rf power is to be led through the two semicircular coupling holes on the cathode mount plate. A heater lead wire is set in the cathode mount plate to supply a dc power to the cathode heater in the inner rod of the coax behind the thermionic cathode.

The rf coupler design was carried out by use of a 3-D electromagnetic field solver. The geometrical parameters, t, w and L in Fig. 6 were determined so that the resonant frequency f_0 and the coupling coefficient β are the designed values, f_0 = 2856 MHz and β = 20, which were determined in our earlier numerical studies [11].

NUMERICAL EVALUATION OF BACK-BOMBARDMENT EFFECT

Cathode Current Increase due to Electron Back-Bombardment in Conventional RF Gun

Figure 7(a) shows calculated heat deposition distributions due to electron back-bombardment onto the cathode in the conventional rf gun. The energy distribution of the back-streaming electrons onto the cathode was given by the 2-D PIC simulations [10]. Stopping ranges of electrons in W and LaB_6 cathodes were then calculated based on an empirical formula given in ref. 13.

The heat distribution in the cathode consists of three components; (i) the highest peak at the cathode surface induced by low energetic electrons back-streaming in the very vicinity of the cathode surface, (ii) the second component seen in Fig. 7(a) corresponding to electrons back-streaming in the 1st rf cavity with incident energies less than 1 MeV, which is eventually found to dominate the cathode surface temperature rise, and (iii) the heat deposited further deep in the cathode by highly energetic electrons from the downstream rf cavities, which is found to make a negligible contribution to the cathode surface temperature rise.

In Fig. 7(a), the second component (ii) is seen more diffuse deep in LaB_6 cathode than in W because of longer stopping ranges of electrons in LaB_6. As the result, the cathode temperature rise, and the corresponding increase of beam current density from the cathode surface are seen to be more rapid in W cathode in Fig. 7(b) by the 1-D time-dependent code in ref. 6.

It is to be noted that, in these calculations, the initial current density on the cathode was set as $J_{c,0}$ = 30 A/cm^2 for both W and LaB_6, and as a consequence the initial cathode temperatures are different.

Comparison between Conventional and Triode RF Guns

Figure 8 shows calculated heat distribution in the cathode and time evolution of beam current density from the cathode surface, comparing three cases, namely use of LaB_6 cathode in the conventional and triode rf guns, and W cathode in the triode rf gun.

In the triode rf gun, the second component (ii) is seen suppressed successfully in Fig. 8(a). As the result, the cathode surface current density dose not increase very rapidly in the triode rf gun as seen in Fig. 8(b).

The first component (i) in the very vicinity of the cathode surface is found to remain as high as in the conventional rf gun. Consequently, the component (i) is found to dominate the cathode surface temperature rise in the triode rf gun, in contrast with the dominant second component (ii) in the conventional rf gun. As the result, unlike in the conventional rf gun, the use of W cathode is found to result in slower temperature rise than LaB_6 cathode, mainly because of higher heat conductivity in W

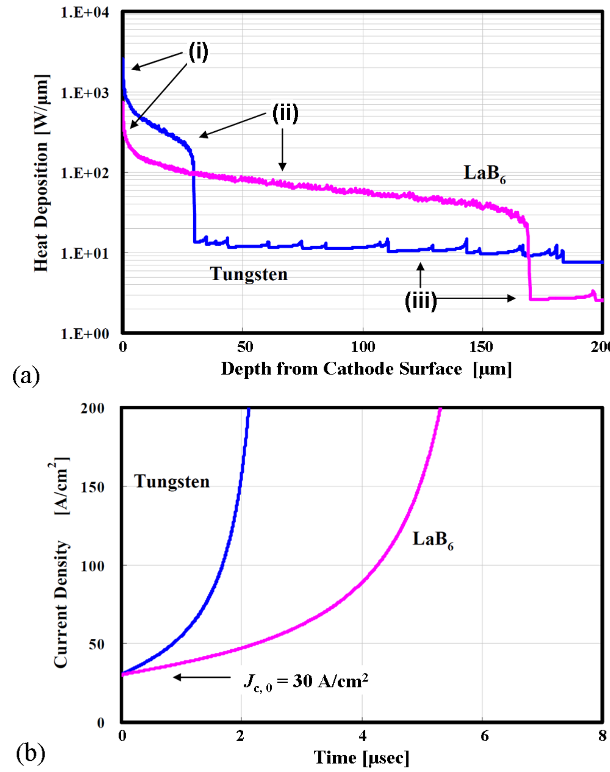

Figure 7: (a) Calculated heat distributions in W and LaB_6 cathodes due to back-bombardment and (b)time evolution of surface current density in the conventional rf gun.

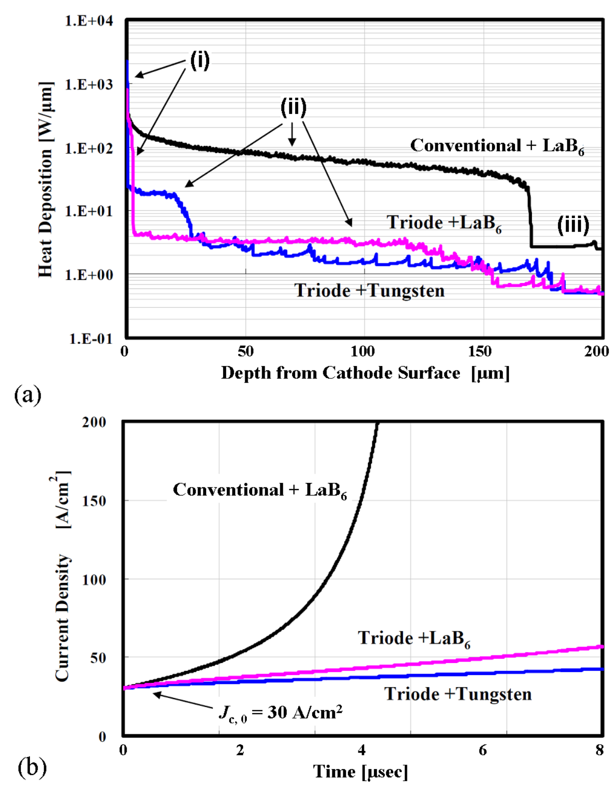

Figure 8: (a) Calculated cathode heat distribution in the cathode and (b) time evolution of surface current density in the conventional and triode rf guns.

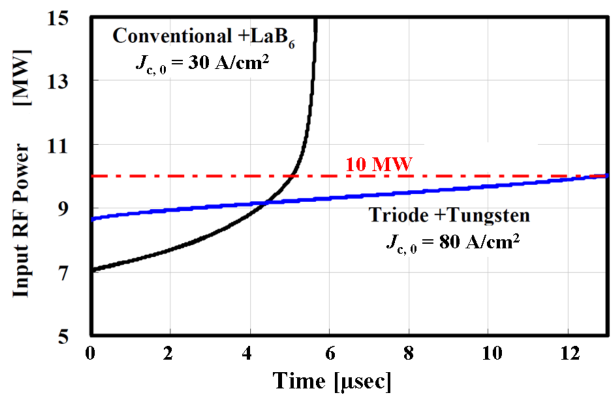

Figure 9: Calculated temporal macro-pulse shapes of rf input required for keeping the output beam energy constant at 7 MeV, comparing the conventional rf gun with an initial cathode current density $J_{c,0}$ = 30 A/cm^2 and the triode rf gun with a higher cathode current $J_{c,0}$ = 80 A/cm^2.

Table 1: Calculated properties of output beams by conventional and triode rf guns.

	Conventional (LaB_6)		Triode (W)
current density [A/cm^2]	**30**	**80**	**80**
peak current [A]	9.8	17	180
norm. emittance [πmm mrad]	2.0	2.5	1.6
back-bombardment power [kW]	18	36	3.6
macro-pulse duration [μsec]	5.1	1.3	13

cathode. We thus decided to use the W cathode for the triode rf gun (see photo in Fig. 4).

Although the rapid beam current increase seen in the conventional rf gun is found to suppressed successfully, the input rf control method [6] is mandatory even in the triode rf gun in order to compensate the temporal energy change due to the residual beam current increase.

Figure 9 shows comparison of temporal macro-pulse shape of rf input required for keeping the output beam energy constant at 7 MeV. The horizontal dashed line represents the maximum available rf input of 10 MW in our experimental setup. As seen in the figure, achievable macro-pulse duration by the conventional rf gun is limited at ~5 μsec with the initial cathode current density $J_{c,0}$ = 30 A/cm^2. In the triode rf gun, a longer macro-pulse duration ~ 13 μsec is expected even with a higher cathode current density $J_{c,0}$ = 80 A/cm^2.

Table 1 summarizes the numerical comparisons between the conventional and triode rf guns. The peak current, emittance and back-bombardment power listed in the table are those at t = 0 for the given initial current densities of $J_{c,0}$ = 30 and 80 A/cm^2 on the cathode surface.

CONCLUSION

The thermionic triode rf gun has been designed. The rf coupler geometry of the short-gap coaxial cavity was designed based on the cavity parameters decided in our earlier numerical studies. Fabrication of the coaxial cavity, the rf coupler, and a tungsten cathode with a wehnelt electrode has been finished. The cold testing and conditioning of the coaxial cavity is under way.

Numerical simulations have shown promising performance of the triode rf gun. A significant reduction of back-bombardment power incident onto the cathode is found numerically to enable twice as long macro-pulse operation with an enhanced peak current of the output beam. These predicted beam properties could contribute to FEL performance improvement to a great extent.

REFERENCES

[1] C.B. McKee, et al., Nucl. Instrum. Methods Phys. Res. A 296 (1990) 716.
[2] T. Kii, et al., Nucl. Instrum. Methods Phys. Res. A 475 (2001) 588-592.
[3] K.Masuda, et al., Nucl. Instrum. Methods Phys. Res. A 483 (2002) 315-320.
[4] T. Kii, et al., Nucl. Instrum. Methods Phys. Res. A 507 (2003) 340-344.
[5] F. Li, et al., Nucl. Instrum. Methods Phys. Res. A 407 (1998) 332-337.
[6] T. Kii, et al., Proc. 9th Int. Conf. Synchrotron Radiation Instrumentation, AIP, 2006, vol. 879, pp. 248–251.
[7] H. Zen, et al., IEEE Trans. Nuclear Sci. 56-3 (2009) 1487-1491.
[8] K. Kanno, et al., Japanese Journal Applied Phys., 41-1 (2002) 62-64.
[9] K. Masuda, et al., Proc. FEL 2006, pp. 656-660.
[10] K. Masuda, PhD thesis Kyoto Univ., 1997.
[11] T. Shiiyama, et al., Proc. FEL 2007, pp. 398-401.
[12] H. Ohgaki, et al., Japanese Journal Applied Phys., 47-10 (2008) 8091–8094.
[13] T. Tabata, et al., Nucl. Instrum. Methods 103 (1972) 85-91.